J Solid State Electrochem (2015) 19:2431–2438
DOI 10.1007/s10008-015-2893-9

ORIGINAL PAPER

Electrochemical DNA sensor for *Staphylococcus aureus* nuc gene sequence with zirconia and graphene modified electrode

Wei Sun[1] · Xiuli Wang[2] · Wencheng Wang[1] · Yongxi Lu[2] · Jingwen Xi[1] · Wen Zheng[2] · Fan Wu[1] · Huilong Ao[1] · Guangjiu Li[2]

Received: 8 October 2014 / Revised: 13 May 2015 / Accepted: 15 May 2015 / Published online: 27 May 2015

Abstract In this paper, zirconia (ZrO_2) and graphene (GR) nanocomposite was electrodeposited on the surface of carbon ionic liquid electrode (CILE), which was used to construct an electrochemical DNA biosensor. GR was electroreduced from graphene oxide by potentiostatic method, and ZrO_2 nanoparticle was further electrodeposited on GR/CILE by cycling voltammetric scan in a $ZrOCl_2$ solution. The presence of GR on the electrode surface can provide a highly conductive interface with large surface area for the loading of ZrO_2 nanoparticles. Single-stranded DNA (ssDNA) probe sequences with phosphate group at the 5′ end could be easily immobilized on the surface of ZrO_2/GR/CILE due to the strong affinity between ZrO_2 and phosphate groups. The ssDNA/ZrO_2/GR/CILE was applied to hybridize with the target ssDNA sequence, and methylene blue (MB) was used as the electrochemical indicator. Due to the different binding models of MB with double-stranded DNA and ssDNA on the electrode surface, electrochemical response of MB was decreased after the hybridization reaction. Under the optimal conditions, the reduction peak current of MB was proportional to the concentration of *Staphylococcus aureus* nuc gene sequence in the range from 1.0×10^{-13} to 1.0×10^{-6} mol L^{-1} with the detection limit of 3.23×10^{-14} mol L^{-1} (3σ). The electrochemical DNA sensor exhibited good selectivity to various mismatched ssDNA sequences, and the polymerase chain reaction amplification products of *S. aureus* nuc gene sequence were further detected with satisfactory results. Therefore, this electrochemical DNA sensor with ZrO_2 nanoparticles and GR nanosheet modified electrode could be used for the detection of specific ssDNA sequence in real biological samples.

Keywords Zirconia nanoparticles · Graphene · Carbon ionic liquid electrode · *Staphylococcus aureus* nuc gene · Electrochemical DNA biosensor

✉ Wei Sun
swyy26@hotmail.com

✉ Guangjiu Li
lgjqust@126.com

[1] College of Chemistry and Chemical Engineering, Hainan Normal University, Haikou 571158, People's Republic of China

[2] College of Chemistry and Molecular Engineering, Qingdao University of Science and Technology, Qingdao 266042, People's Republic of China

Introduction

As a new kind of two-dimensional carbon nanomaterials, graphene (GR) exhibits many advantages such as extremely high thermal conductivity, good mechanical strength, high mobility of charge carriers, big specific surface area, and upstanding electrical properties [1, 2]. Since the discovery of GR at 2004 [3], great efforts have been made to investigate the synthesis and application of GR in different fields [4, 5]. Due to its unique electronic properties, large surface area, and good electrochemical stability, GR had been intensively studied in electrochemistry and electrochemical sensors [6, 7]. Because GR has a large two-dimensional surface, it is often used as the building unit for the preparation of nanocomposite. Various nanomaterials with different morphologies can be loaded on the GR nanosheet. Singh reviewed the synthesis of GR-based nanocomposite [8], which exhibited the synergistic effects with the applications in solar cell, biosensor, Li-ion battery. Bai et al. presented a review about the synthesis and application of GR-inorganic nanocomposites [9]. The presence of various nanomaterials on the surface of GR nanosheets can

result in a specific hybrid with multi-functions due to the synergistic properties originated from the individual components and their interaction.

Zirconia (ZrO_2) is an inorganic oxide with the properties such as thermal stability, chemical inertness, resistance to poisoning, strong affinity for phosphoric group, large surface area, lack of toxicity and affinity for oxygen-containing groups [10], which is often used for the immobilization of biomolecules with oxygenal groups [11]. Electrochemical sensors with ZrO_2 nanomaterials have been reported. Liu et al. used ZrO_2 nanoparticles as selective sorbents for the electrochemical detection of organophosphate pesticides and nerve agents [12]. Du et al. developed a ZrO_2 nanoparticle-modified electrode for the sensitive electrochemical stripping voltammetric detection of organophosphate compounds [13]. Zong et al. prepared a ZrO_2-grafted collagen for the immobilization of redox proteins and applied to unmediated biosensing of H_2O_2 [14]. Liu et al. studied the direct electrochemistry and thermal stability of Hb immobilized on ZrO_2 nanoparticle-modified pyrolytic graphite electrode [15]. Yang et al. reported the direct electron transfer of glucose oxidase on ZrO_2 nanoparticle-modified electrode [16]. Qiao et al. investigated the direct electron transfer and electrocatalysis of myoglobin in poly(ethylene glycol) and ZrO_2 nanoparticle layer-by-layer films [17]. Also, ZrO_2-modified electrode can be used for the fabrication of electrochemical DNA sensors due to the strong affinity with the phosphate groups present at the 5′ end of single-stranded DNA (ssDNA) probes. Zhu et al. applied a ZrO_2-modified gold electrode for the electrochemical detection of DNA hybridization [18]. Yang et al. electrodeposited ZrO_2 on the composite film-modified electrode and used in electrochemical DNA sensor for the detection of PAT gene fragment [19].

Recently, the nanocomposite based on the integration of GR and ZrO_2 has been reported and used for the electrochemical detection, which exhibits the synergistic effects. Pang et al. synthesized ZrO_2 nanostructures on graphene oxide plane and further used for highly selective capture of phosphopeptides [20]. Du et al. described a one-step electrodeposition method for GR-ZrO_2 nanocomposite-modified glassy carbon electrode and used for the detection of organophosphorus agents [21]. Gong et al. proposed a one-step co-electrodeposition of ZrO_2 nanoparticle-decorated GR hybrid nanosheets for an enzymeless parathion sensor [22]. Sun et al. also applied a GR-ZrO_2 nanocomposite-modified electrode for the simultaneous electrochemical determination of guanosine and adenosine [23].

In recent years, electrochemical DNA sensors have been developed greatly, which exhibits the advantages such as high sensitivity, rapid speed, wide dynamic range, and low cost with miniaturized and automated devices [24]. Due to the specific characteristics of nanomaterials including large surface area, good biocompatibility, and high electrochemical conductivity, nanoparticle-based electrochemical interfaces have been devised for the ssDNA immobilization [25]. Drummond et al. reviewed the development and application of DNA-based electrochemical sensor [26]. Hvastkovs et al. summarized the recent advances in electrochemical DNA hybridization detection [27]. Liu et al. reviewed the development of electrochemical DNA biosensors and the future prospects [28]. Electrochemical DNA sensors have been used in food safety monitoring and the detection of pathogen DNA. Tichoniuk et al. described an electrochemical DNA biosensor for the detection of *Aeromonas hydrophila* with a mixed self-assembled monolayer-modified electrode [29]. Ligaj et al. presented two kinds of electrochemical DNA sensor for the detection of pathogenic bacteria [30]. Fernandes et al. reported the construction of electrochemical genosensor based on multi-walled carbon nanotube-chitosan-bismuth and lead sulfide nanoparticle for the detection of pathogenic *Aeromonas* [31]. Our group applied an electrochemical DNA sensor based on carboxyl-functionalized graphene oxide and poly-L-lysine-modified electrode for the detection of *tlh* gene sequences that related to *Vibrio parahaemolyticus* [32]. Also, a dendritic nanogold and electrochemically reduced graphene-modified electrode were prepared for the detection of specific DNA sequence of *Listeria monocytogenes* [33]. Therefore, electrochemical DNA sensor with nanomaterials has the potential applications for the detection of various pathogens.

In this paper, GR-ZrO_2 nanocomposite was employed for the construction of an electrochemical DNA sensor. By using ionic liquid (IL) as the modifier/binder in the traditional carbon paste electrode, carbon ionic liquid electrode (CILE) had been proved to exhibit many advantages such as high conductivity, wide electrochemical window, good electrocatalytic activity, low cost, easy preparation, antifouling effect, and renewable surface [34, 35]. The GR-ZrO_2 nanoparticle-modified CILE was fabricated for the DNA immobilization and electrochemical detection, which exhibited a synergistic augmentation of the electrochemical response to the indicator. GR can provide a large surface area with high conductivity, which is a benefit for the loading of ZrO_2 nanoparticles and the electron transfer between methylene blue (MB) and the electrode. While the presence of ZrO_2 nanoparticles has a high affinity to the phosphate group of ssDNA sequence, which can result in the formation of stable ssDNA-modified electrode. The procedure for the preparation of this electrochemical DNA sensor was illustrated in Scheme 1. The fabricated electrochemical DNA sensor was used to the detection of *Staphylococcus aureus* nuc gene sequence with high sensitivity and good stability.

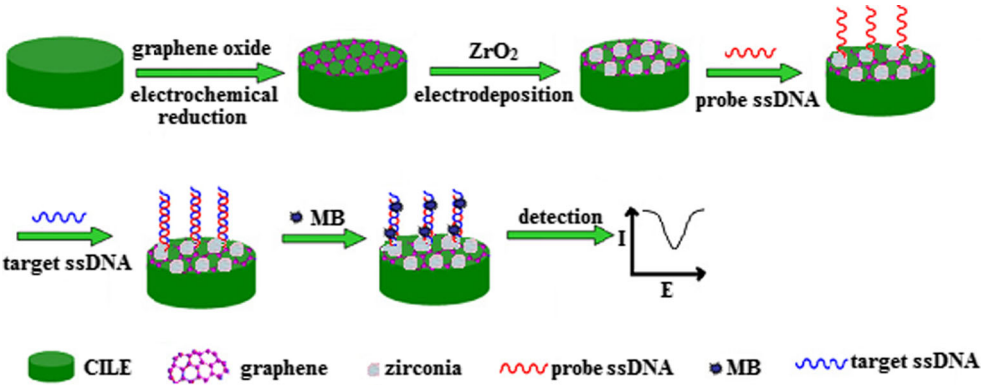

Scheme 1 A schematic representation of the preparation procedure of this electrochemical DNA biosensor

Experimental

Apparatus and reagents

A CHI 750B electrochemical workstation (Shanghai CH Instrument, China) was used to carry out all the electrochemical experiments such as cyclic voltammetry (CV) and differential pulse voltammetry (DPV). A conventional three-electrode system, which was composed of a saturated calomel electrode (SCE) as reference electrode, a platinum wire as auxiliary electrode, and a homemade modified CILE as working electrode (Φ=4 mm), was employed throughout the experiments. The DNA extraction kit was purchased from Beijing Tiangen Biotech. Ltd. Co. (China), and the polymerase chain reaction (PCR) was performed on an Eppendorf Mastercycler Gradient PCR system (Eppendorf, Germany). Scanning electron microscopy (SEM) was obtained by a JSM-7100F scanning electron microscope (Japan Electron Company, Japan).

1-Hexylpyridinium hexafluorophosphate ($HPPF_6$; >99 %, Lanzhou Greenchem. ILS. LICP. CAS., China), graphite powder (Shanghai Colloid Chemical Plant, particle size≤30 μm, China), graphene oxide (GO; Taiyuan Tanmei Co., China), $ZrOCl_2{\cdot}8H_2O$ (Tianjin Bodi Chem. Ltd. Co., China), and methylene blue (MB; Shanghai Chemicals Plant, China) were used as received. Different kinds of buffers used were listed as follows: 0.2 mol L^{-1} phosphate-buffered saline (PBS; pH 8.0), 50.0 mmol L^{-1} PBS (pH 7.0), 50.0 mmol L^{-1} Tris-HCl buffer solution (pH 7.0), 1× TAE buffer (40.0 mmol L^{-1} Tris+1.0 mmol L^{-1} EDTA+40.0 mmol L^{-1} acetate, pH 8.0). All the solutions were prepared with doubly distilled water, and other chemicals used were of analytical reagents grade.

All the ssDNA sequences were purchased from Shanghai Sangon Biological Engineering Tech. Ltd. Co. (China). The 22-base ssDNA sequences that selected from *S. aureus* nuc gene sequence were listed as follows:

Probe ssDNA sequence: 5′-TGG ACG TGG CTT AGC GTA TAT T-3′

Target ssDNA sequence: 5′-AAT ATA CGC TAA GCC ACG TCC A-3′

One-base mismatched ssDNA sequence: 5′-AAG ATA CGC TAA GCC ACG TCC A-3′

Three-base mismatched ssDNA sequence: 5′-AAG ATA CGC TAC GCC ACG TCT A-3′

Non-complementary ssDNA sequence: 5′-GCG GTT GAA TCG GCG ATG GGT GA-3′

The specific ssDNA sequence from other kinds of pathogens such as *tlh* gene sequence of *V. parahaemolyticus* (5′-TCGTCGCATCTGGCAGTGTCATC-3′) and *hly* gene sequence of *L. monocytogenes* (5′-TGCAGTGACAAATGTG CCGCCA-3′) was used in the experiment to testify the selectivity.

The DNA template was extracted from *S. aureus* strains by the DNA extraction kit with the recommended procedure and purified for the PCR amplification. The oligonucleotide primers for PCR amplification reaction of *S. aureus* nuc gene were selected with the following sequences:

Primer F: 5′-CCT GAA GCA AGT GCA TTT ACG A-3′

Primer R: 5′-CTT TAG CCA AGC CTT GAC GAA CT-3′

Fabrication of ZrO_2/GR/CILE

CILE was fabricated based on the reported procedure [36]. In brief, 1.6 g of graphite powder and 0.8 g of $HPPF_6$ were mixed thoroughly in a mortar to get the IL-modified carbon paste, which was inserted into a glass tube (Φ=4 mm) tightly with a copper wire as an electrical contact. The surface of CILE was smoothed on a piece of weighing paper just before use for the further modification. Then the newly prepared CILE was put into a 1.0 mg mL^{-1} GO solution, and electroreduction was performed at the potential of −1.3 V for 600 s to get the GR-modified CILE. ZrO_2 nanoparticles were further electrodeposited on the surface of GR/CILE by cyclic voltammetry with the potential range from −1.1 to 0.7 V at the scan rate of

20 mV s^{-1} in a 5.0 mmol L^{-1} $ZrOCl_2$ and 0.1 mol L^{-1} KCl mixture solution. The modified electrode was denoted as ZrO_2/GR/CILE, and other kinds of modified electrodes including GR/CILE and ZrO_2/CILE were prepared by the similar procedure for comparison.

Preparation of electrochemical DNA sensor

A 10.0 μL of 1.0×10^{-6} mol L^{-1} probe ssDNA sequence solution (in 50.0 mmol L^{-1} pH 7.0 PBS) was casted directly onto the surface of ZrO_2/GR/CILE. Due to the presence of phosphate group in the 5′ end of the ssDNA probe sequence and the strong affinity of ZrO_2 with the phosphate group, probe ssDNA sequence can be tightly immobilized on the surface of ZrO_2/GR/CILE. Then the electrode was washed with 0.5 % sodium dodecyl sulfate (SDS) solution and doubly distilled water for three times successively to remove the unabsorbed probe ssDNA sequence on the electrode surface. This probe ssDNA-captured electrode was denoted as ssDNA/ZrO_2/GR/CILE.

Hybridization reaction

The efficient drop hybridization procedure was used for the detection of target ssDNA sequence, which was hybridized with the probe ssDNA-modified electrode. After dropping 8.0 μL of target ssDNA sequence (in 50.0 mmol L^{-1} PBS) directly onto the surface of ssDNA/ZrO_2/GR/CILE, which was inverted upside down to hold the solution, the hybridization reaction between the target ssDNA sequence in the solution and the probe ssDNA sequence on the electrode surface was allowed to proceed for 20 min at room temperature. Then the electrode was washed with 0.5 % SDS solution and doubly distilled water for three times to remove the unhybridized target ssDNA sequence. This hybridized electrode was named as dsDNA/ZrO_2/GR/CILE.

Electrochemical detection

The hybridized electrode was immersed into a 2.0×10^{-5} mol L^{-1} MB solution for 10 min to accumulate MB molecules on the electrode surface and then washed by 50.0 mmol L^{-1} PBS for three times. After that, the electrode was immersed in a 50.0 mmol L^{-1} Tris-HCl buffer solution (pH 7.0), and the electrochemical response of MB was measured by DPV method with the instrumental parameters set as the following: pulse amplitude 0.008 V, pulse width 0.05 s, and pulse period 0.2 s.

PCR amplification of *Staphylococcus aureus* nuc gene

Amplification of nuc gene fragments was carried out in a final volume of 25 μL in 0.2 mL tube containing 200.0 nmol L^{-1} each primer of nuc primer F and primer R; 10× reaction buffer B, 2.0 mmol L^{-1} $MgCl_2$; 200.0 nmol L^{-1} each of dATP, dCTP, dGTP, and dTTP; 1.5 units of Taq DNA polymerase; and 1.0 μL DNA template purified from samples. During the PCR procedure, DNA was initially denatured at 94 °C for 30 s. PCR conditions were optimized as follows: 35 cycles of amplification (94 °C for 30 s, 56 °C for 30 s, 72 °C for 30 s) and final extension at 72 °C for 5 min. The concentration of PCR product was further detected by agarose gel electrophoresis separation with UV-Vis spectroscopic determination. The PCR products without DNA template were used as comparison, and all the products were prepared and kept at 4 °C just before use.

After amplification, the PCR product was diluted with 20.0 mmol L^{-1} PBS (pH 7.0), denatured in a boiling water bath for 10 min, and then immediately cooled in an ice water bath for 2 min. According to the previous procedure of hybridization and electrochemical detection, the *S. aureus* nuc gene PCR amplification product was detected by differential pulse voltammetry.

Results and discussion

SEM of the modified electrode

Figure 1 showed the SEM images of GR/CILE and ZrO_2/GR/CILE. After electrodeposition of GR on CILE, the typical lamellar structure of GR could be observed (Fig. 1a), which was highly beneficial in maintaining a large electrode surface. Electrochemical reduction of GO has been proved to be a facial and controllable method to synthesize GR nanosheets directly on the electrode surface, and the GR-modified electrode exhibits enhanced electrochemical performances with increased surface area [37]. While on ZrO_2/GR/CILE, (Fig. 1b) ZrO_2 nanoparticles could be observed on the surface of electrode with the average diameters of 100 nm. Electrodeposition has been proved to be an effective method for the synthesis of ZrO_2 nanoparticles with high stability [18], and the presence of ZrO_2 nanoparticles can provide more attachment sites for the adsorption of probe ssDNA sequence.

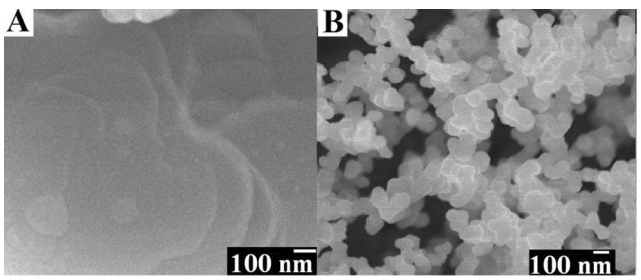

Fig. 1 SEM images of GR/CILE (**a**) and ZrO_2/GR/CILE (**b**)

Electrochemical characterization of the modified electrodes

Cyclic voltammetric technique has been widely used as an effective tool to measure the current changes of the working electrode during the modified procedure. Cyclic voltammetric behaviors of different modified electrodes were recorded in a 1.0 mmol L^{-1} $[Fe(CN)_6]^{3-/4-}$ solution with the voltammograms shown in Fig. 2. On bare CILE, the redox peak current was the smallest (curve a). When GR was electroreduced and present on the CILE surface, the redox peak current turned to maximum value (curve c), which could be ascribed to the formation of highly conductive GR on the electrode surface. Electroreduction is an efficient and green procedure for the synthesis of GR nanosheets directly on the electrode surface without the usage of hazardous reagents [37]. Due to the specific characteristics of GR such as large surface area, small bandgap, excellent electrical conductivity, high electron transfer capacity and low electrochemical noise, the presence of GR on the electrode can accelerate electrochemical reaction rate, increase the effective area of electrode, and accelerate the diffusional rate of $[Fe(CN)_6]^{3-/4-}$ to the electrode. Therefore, a good response of $[Fe(CN)_6]^{3-/4-}$ appeared on GR-modified electrode. After ZrO_2 nanoparticles were further decorated on the surface of GR/CILE, the redox peak current decreased (curve b) and was smaller than that of GR/CILE, which may be ascribed to the formation of semiconductive ZrO_2 nanoparticles on the electrode surface. Electrodeposition is a commonly adopted way to fabricate the nanomaterial, and ZrO_2 nanoparticles can be directly formed on the electrode surface [18]. The presence of semiconductive ZrO_2 nanoparticles on the electrode can hinder the electron transfer of $[Fe(CN)_6]^{3-/4-}$ and result in the decrease of the redox peak currents correspondingly. The effective electrode surface area can be calculated by the Randles-Servick equation: $I_p=(2.69\times 10^5)n^{3/2}AD_0^{1/2}\upsilon^{1/2}C_0$, where I_p is the redox peak current (A), n is the electron transfer number, A is the effective surface area (cm^2), D_0 is the diffusional coefficient of $K_3[Fe(CN)_6]$ in the solution ($cm^2\ s^{-1}$), C_0 is the concentration of $K_3[Fe(CN)_6]$ (mol L^{-1}), and υ is the scan rate (V s^{-1}). Cyclic voltammograms of different electrodes in a 1.0 mmol L^{-1} $K_3[Fe(CN)_6]^{3-/4-}$ solution at different scan rates were recorded. Based on the above equation, the effective surface area of CILE, GR/CILE, and ZrO_2/GR/CILE could be calculated as 0.164, 0.278, and 0.181 cm^2, respectively. Therefore, the presence of GR nanosheets on the electrode surface can greatly increase the surface area, and the further decoration of semiconductive ZrO_2 nanoparticles decreases the effective surface.

Electrochemical behaviors of MB on different ssDNA-modified electrodes

MB is a phenothiazine dye that has been widely used as electrochemical indicator in DNA biosensor, which can interact with ssDNA or dsDNA by different binding models. MB can interact with phosphate framework of ssDNA by electrostatic binding, or intercalate with major or minor helix grooves of dsDNA, or bind specifically to the guanine bases on DNA molecules. And the binding model is greatly influenced by the experimental conditions. Figure 3 showed differential pulse voltammograms of MB on different ssDNA-modified electrodes. The reduction peak current of MB on ssDNA/GR/CILE (curve b) was larger than that of ssDNA/CILE (curve a), indicating that the highly conductive GR on the electrode surface was benefit for the electron transfer of MB. The reduction peak current of MB on ssDNA/ZrO_2/CILE (curve c) was also larger than that of ssDNA/CILE (curve a), indicating that the presence of ZrO_2 nanoparticles on the electrode surface could absorb more ssDNA molecules due to its strong affinity with the phosphoric groups in ssDNA structure. The biggest reduction peak current of MB appeared on ssDNA/ZrO_2/GR/CILE, indicating the synergistic effects of GR and

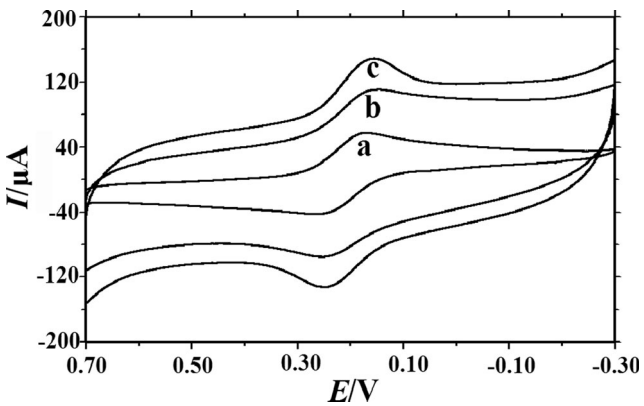

Fig. 2 Cyclic voltammograms of CILE (*a*), ZrO_2/GR/CILE (*b*), and GR/CILE (*c*) in a 1.0 mmol L^{-1} $[Fe(CN)_6]^{3-/4-}$ and 0.5 mol L^{-1} KCl solution with the scan rate of 100 mV s^{-1}

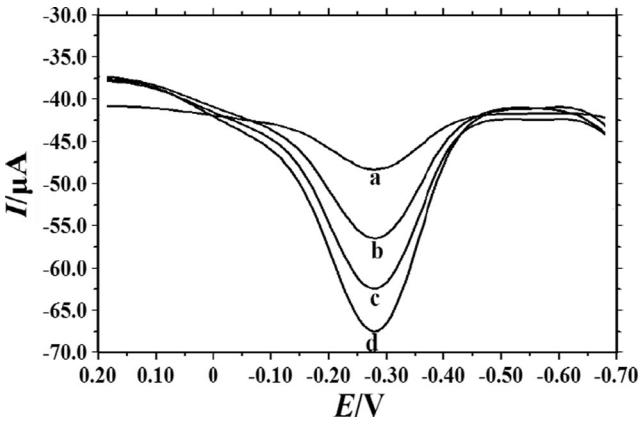

Fig. 3 Differential pulse voltammograms of ssDNA/CILE (*a*), ssDNA/GR/CILE (*b*), ssDNA/ZrO_2/CILE (*c*), and ssDNA/ZrO_2/GR/CILE (*d*) using MB as the indicator in 50.0 mmol L^{-1} pH 7.0 Tris-HCl buffer solution

ZrO_2 nanoparticles on the electrode. GR exhibits high conductivity with large surface area, which can facilitate the electron transfer and provide more sites for the deposition of ZrO_2 nanoparticles. More ZrO_2 nanoparticles that formed on the electrode surface can adsorb more ssDNA sequences on the electrode. Then the concentration of MB molecules was further increased due to the interaction with guanine bases on the ssDNA structure. Therefore, the electrochemical responses of MB were enhanced on ssDNA/ZrO_2/GR/CILE with the biggest reduction peak current appearance.

Optimization of hybridization time

The hybridization time of probe ssDNA on the electrode surface with the target ssDNA in the solution was investigated by recording the reduction peak current of MB after different hybridization time. The result indicated that the current value increased from 0 to 20 min and then changed slowly, which exhibited the completely hybridization. Therefore, 20 min was selected through the experiment.

Selectivity of the electrochemical DNA biosensor

Figure 4 showed the reduction peak currents of MB on different electrodes that hybridized with various target ssDNA sequences. The biggest value appeared at the probe ssDNA/ZrO_2/GR/CILE without hybridization (signal a), which was due to the interaction of MB with guanine groups of ssDNA on the electrode. While the similar values appeared on the hybridized electrodes with non-complementary ssDNA sequence (signal b), *tlh* gene sequence of *V. parahaemolyticus* (signal c), and *hly* gene sequence of *L. monocytogenes* (signal d), which indicated that no hybridization reaction took place and the amount of ssDNA sequence on the electrode surface remained almost constant. Therefore, the electrochemical responses remained unchanged. As for the three-base mismatched ssDNA sequence (signal e) and one-base mismatched ssDNA sequence (signal f), the peak currents decreased to 36.6 and 54.9 % as compared with that of background response, indicating the partly formation of dsDNA structure on the electrode surface after hybridization, while the smallest value appeared at the electrode that hybridized with the complementary ssDNA sequence (signal g). The presence of duplex structure on the electrode surface after hybridization prevented the interaction of MB with the guanine residues of the probe ssDNA sequence. And less MB molecules existed on the electrode surface with the decrease of reduction peak current appearance. It is worthy to note that the reduction peak current after hybridization with three-base mismatched ssDNA sequence was higher than that with one-base mismatched ssDNA sequence, which demonstrated this DNA biosensor exhibited high selectivity and good distinguish ability for the hybridization detection of different ssDNA sequences.

Sensitivity of the electrochemical DNA biosensor

The sensitivity of this electrochemical DNA sensor was investigated by using the probe ssDNA sequence-modified electrode to hybridize with different concentrations of the complementary target ssDNA sequence and the typical differential pulse voltammograms were shown in Fig. 5. The more the hybridization of probe ssDNA sequence with target ssDNA sequence, the large amounts of dsDNA formed on the electrode surface, the less MB molecules interacted with guanine groups, and the smaller electrochemical response of MB could be observed under the optimal conditions. The reduction peak current of MB decreased with the concentration of

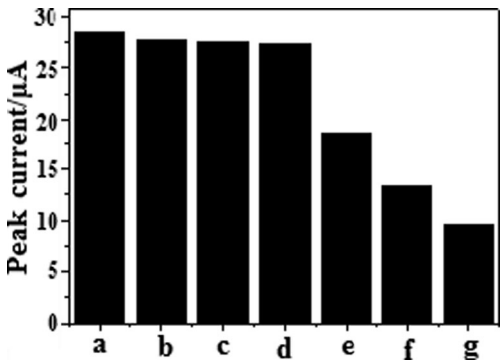

Fig. 4 Comparison of the current value of 2.0×10^{-5} mol L^{-1} MB on ssDNA/ZrO_2/GR/CILE (*a*), after electrodes hybridized with non-complementary (*b*), *tlh* gene sequence of *Vibrio parahaemolyticus* (*c*), *hly* gene sequence of *Listeria monocytogenes* (*d*), three-base mismatched ssDNA sequence (*e*), one-base mismatched ssDNA sequence (*f*), and complementary ssDNA sequence (*g*)

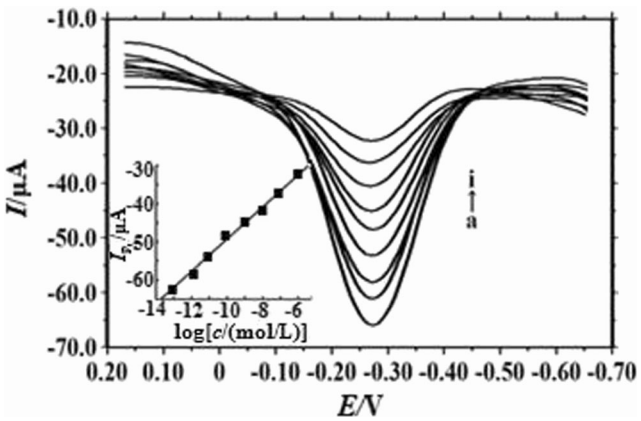

Fig. 5 Differential pulse voltammograms of MB on ssDNA/ZrO_2/GR/CILE after hybridization with different concentrations of target ssDNA sequence (from *a* to *i* were 0, 1.0×10^{-13}, 1.0×10^{-12}, 1.0×10^{-11}, 1.0×10^{-10}, 1.0×10^{-9}, 1.0×10^{-8}, 1.0×10^{-7}, and 1.0×10^{-6} mol L^{-1}, respectively). *Inset*: plots of I_p versus logarithm of target ssDNA sequence concentration

complementary target ssDNA sequence in the range from 1.0×10^{-13} to 1.0×10^{-6} mol L^{-1}. The relationship of reduction peak currents with the logarithmic value of the target ssDNA sequence concentration could be plotted with the linear regression equation as $I(\mu A)=2.98\log[c/(\text{mol } L^{-1})]-27.58$ (n=8, γ=0.998). The detection limit was calculated as 3.23×10^{-14} (3σ) (where σ is the standard deviation of the blank solution, n=11), which was lower than some previous reported values such as chitosan/Fe_3O_4 microsphere-GR composite-modified CILE (3.59×10^{-13} mol L^{-1}) [38], ZrO_2 nanoparticle-modified gold electrode (1.0×10^{-10} mol L^{-1}) [18], multi-walled carbon nanotubes/ZrO_2/chitosan-modified glassy carbon electrode (7.5×10^{-11} mol L^{-1}) [39], and multi-walled carbon nanotubes and gold nanoparticle-modified gold electrode (7.5×10^{-12} mol L^{-1}) [40]. The relative standard deviation (RSD) of the reduction peak current for the six repeated detections of 1.0×10^{-7} mol L^{-1} target ssDNA sequence was calculated as 4.1 %, indicating the good reproducibility of this proposed method. The stability of ssDNA/ZrO_2/GR/CILE was investigated after 10 days storage at 4 °C and further used to hybridize with the target ssDNA sequence; 95.8 % of the initial current responses remained, indicating this modified electrode exhibited good stability as electrochemical DNA biosensor for the ssDNA detection.

Detection of PCR products of *S. aureus* nuc gene sequence

The PCR products were pretreated by heating denaturation to obtain the ssDNA solution, which were further analyzed by the proposed method. The concentration of PCR product was estimated by UV-Vis absorption spectrophotometry with the value of 391.0 ng μL^{-1}, which was further treated by heating to get the denatured ssDNA sequences. Then the ssDNA solution was detected by the proposed method. By dropping 6.0 μL sample of ssDNA solution on the surface of ssDNA/ZrO_2/GR/CILE with the following hybridization and electrochemical detection performed under the optimal conditions, the reduction peak current was recorded and shown in Fig. 6. The smallest reduction peak current appeared on ZrO_2/GR/CILE (curve a), which was ascribed to the electrochemical reaction of MB on the modified electrode. While on ssDNA/ZrO_2/GR/CILE (curve c), the biggest electrochemical responses of MB could be observed, which could be attributed to the interaction of MB with guanine groups of ssDNA on the electrode surface that could accumulate more MB. After the hybridization with the PCR-amplified sample, the reduction peak current decreased greatly (curve b), which indicated that more dsDNA molecules were formed on the electrode surface and decreased the amounts of MB on the electrode surface. Therefore, the corresponding decrease of the reduction peak current of MB appeared. This significant difference of the reduction peak current of MB between the probe ssDNA-modified electrode (curve c) and hybridized dsDNA electrode (curve b) also confirmed that this electrochemical DNA biosensor could be effectively applied to detect the PCR product of *S. aureus* nuc gene.

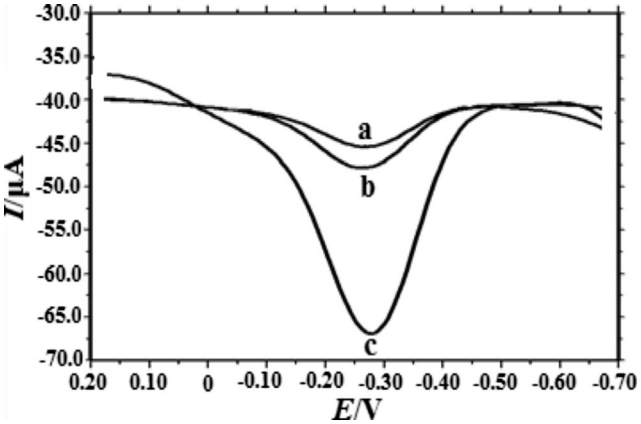

Fig. 6 Differential pulse voltammograms of MB at ZrO_2/GR/CILE (*a*), ssDNA/ZrO_2/GR/CILE hybridized with PCR product of *Staphylococcus aureus* (*b*), and ssDNA/ZrO_2/GR/CILE (*c*)

Conclusions

In this work, GR nanosheets and ZrO_2 nanoparticles were electrodeposited on the surface of CILE to get the modified electrode (ZrO_2/GR/CILE). Due to the strong affinity of ZrO_2 nanoparticles to the phosphate group of ssDNA sequences, probe ssDNA sequence related to nuc gene was immobilized on the surface of ZrO_2/GR/CILE. The presence of electroreduced GR can provide large surface area with higher conductive interface, and electrodeposited ZrO_2 nanoparticles can form a suitable platform for the high loading of probe ssDNA sequence. The presence of GR and ZrO_2 nanoparticles exhibits synergistic effects with high efficiency for the DNA immobilization and electron transfer. The presence of duplex structure on the electrode surface after hybridization prevented the interaction of MB with the guanine residues of the probe ssDNA sequence. And less MB molecules existed on the electrode surface with the decrease of reduction peak current appeared. The *S. aureus* nuc gene sequence was successfully detected by this electrochemical DNA sensor. By using electroactive MB as the hybridization indicator, the target ssDNA sequence can be detected in the concentration range from 1.0×10^{-13} to 1.0×10^{-6} mol L^{-1} with a detection limit as 3.23×10^{-14} mol L^{-1} (3σ). Therefore, the method can be used for the detection of specific DNA sequences with the advantages including better selectivity and higher sensitivity.

Acknowledgments We acknowledge the financial support from the National Natural Science Foundation of China (Nos. 21365010, 51363008), the Natural Science Foundation of Shandong Province (ZR2013BM014), the Natural Science Foundation of Hainan Province

(20152016), and the International Science and Technology Cooperation Project of Hainan Province (KJHZ2015-13).

References

1. Geim AK, Novoselov AK, Novoselov KS (2007) Nat Mater 6:183–191
2. Chen D, Tang LH, Li JH (2010) Chem Soc Rev 39:3157–3180
3. Novoselov KS, Geim AK, Morozov SV, Jiang D, Zhang Y, Dubonos SV, Grigorieva IV, Firsov AA (2004) Science 306:666–669
4. Dreyer DR, Park SJ, Bielawski CW, Ruoff RS (2010) Chem Soc Rev 39:228–240
5. Huang X, Zeng Z, Fan Z, Liu J, Zhang H (2012) Adv Mater 24:5979–6004
6. Brownson D, Banks C (2010) Analyst 135:2768–2778
7. Chen D, Feng HB, Li JH (2012) Chem Rev 112:6027–6053
8. Singh V, Joung D, Zhai L, Das S, Khondaker SI, Seal S (2011) Prog Mater Sci 56:1178–1271
9. Bai S, Shen XP (2012) RSC Adv 2:64–98
10. Dobson KD, McQuillan AJ (1997) Langumuir 13:328–339
11. Fang M, Kaschak DM, Sutorik AC, Mallouk TE (1997) J Am Chem Soc 119:12184–12191
12. Liu GD, Lin YH (2005) Anal Chem 77:5894–5901
13. Du D, Ye XP, Zhang JD, Zeng Y, Tu HY, Zhang AD, Liu DL (2008) Electrochem Commun 10:686–690
14. Zong SZ, Cao Y, Zhou YM, Ju HX (2006) Langmuir 22:8915–8919
15. Liu SQ, Dai ZH, Chen HY, Ju HX (2004) Biosens Bioelectron 19:963–969
16. Yang XD, Zhang QQ, Sun YM, Liu SQ (2007) IEEE Sensors J 12:1735–1741
17. Qiao K, Hu NF (2009) Bioelectrochemistry 75:71–76
18. Zhu NN, Zhang AP, Wang QJ, He PG, Fang YZ (2004) Anal Chim Acta 510:163–168
19. Yang J, Jiao K, Yang T (2007) Anal Bioanal Chem 389:913–921
20. Pang H, Lu QY, Gao F (2011) Chem Commun 47:11772–11774
21. Du D, Liu J, Zhang XY, Cui XL, Lin YH (2011) J Mater Chem 21:8032–8037
22. Gong JM, Miao XJ, Wang HF, Song DD (2012) Sensors Actuators B Chem 102:341–347
23. Sun W, Wang XZ, Sun XH, Deng Y, Liu J, Lei BX, Sun ZF (2013) Biosens Bioelectron 44:146–151
24. Drummond TG, Hill MG, Barton JK (2003) Nat Biotechnol 21:1192–1199
25. Mao X, Liu GD (2008) J Biomed Nanotechnol 4:419–431
26. Bonanni A, Valle M (2010) Anal Chim Acta 678:7–17
27. Hvastkovs EG, Buttry DA (2010) Analyst 135:1817–1829
28. Liu A, Wang K, Weng SH, Lei Y, Lin LQ, Chen W, Lin XH, Chen YZ (2012) Trends Anal Chem 37:101–111
29. Tichoniuk M, Gwiazdowska D, Ligaj M, Filipiak M (2010) Biosens Bioelectron 26:1618–1623
30. Ligaj M, Tichoniuk M, Gwiazdowska D, Filipiak M (2014) Electrochim Acta 128:67–74
31. Fernandes AM, Abdalhai MH, Ji J, Xi BW, Xie J, Sun JD, Noeline R, Lee BH, Sun XL (2015) Biosens Bioelectron 63:399–406
32. Sun W, Zhang YY, Ju XM, Li GJ, Gao HW, Sun ZF (2012) Anal Chim Acta 752:39–44
33. Sun W, Qi XW, Zhang YY, Yang HR, Gao HW, Chen Y, Sun ZF (2012) Electrochim Acta 5:45–151
34. Opallo M, Lesniewski A (2011) J Electroanal Chem 656:2–16
35. Shiddiky MJA, Torriero AAJ (2011) Biosens Bioelectron 26:1775–1787
36. Sun W, Li YZ, Yang MX, Li J, Jiao K (2008) Sensors Actuators B 133:387–392
37. Zhou M, Wang YL, Zhai YM, Zhai JF, Ren W, Wang FA, Dong SJ (2009) Chem Eur J 15:6116–6120
38. Sun W, Qi XW, Chen Y, Liu SY, Gao HW (2011) Talanta 87:106–112
39. Yang YH, Wang ZJ, Yang MH, Li JS, Zheng F, Shen GL, Yu RQ (2007) Anal Chim Acta 594:268–274
40. Ma HY, Zhang LP, Pan Y, Zhang KY, Zhang YZ (2008) Electroanalysis 20:1220–1226